frontiers | Frontiers in Dementia

TYPE Original Research
PUBLISHED 28 October 2024
DOI 10.3389/frdem.2024.1477986

OPEN ACCESS

EDITED BY
Wenzhang Wang,
Case Western Reserve University,
United States

REVIEWED BY
Chunyu Wang,
Central South University, China
Sabina Bhatta,
Case Western Reserve University,
United States

*CORRESPONDENCE
Jinchong Xu
✉ jxu31@jhmi.edu
Chan Hyun Na
✉ cahnhyun@jhmi.edu
Sung-Ung Kang
✉ skang34@jhmi.edu

†These authors have contributed equally to this work and share first authorship
‡These authors have contributed equally to this work and share last authorship

RECEIVED 08 August 2024
ACCEPTED 14 October 2024
PUBLISHED 28 October 2024

CITATION
Akkentli F, Jang Ik, Choi Y, Min Y, Park J, Jo H, Kim L, Mendpara A, Bains B, Yoo D, Xu J, Na CH and Kang S-U (2024) Quantitative proteomic analysis using a mouse model of Lewy body dementia induced by α-synuclein preformed fibrils injection.
Front. Dement. 3:1477986.
doi: 10.3389/frdem.2024.1477986

Quantitative proteomic analysis using a mouse model of Lewy body dementia induced by α-synuclein preformed fibrils injection

Fatih Akkentli[1†], In kyu Jang[1,2†], Yoonseop Choi[1†], Young Min[1], Jinhee Park[1], Heejin Jo[1], Leoni Kim[1], Aashi Mendpara[1,2], Bikram Bains[1,3], Dongyoon Yoo[1], Jinchong Xu[1,4*‡], Chan Hyun Na[1,4*‡] and Sung-Ung Kang[1,4*‡]

[1]Neuroregeneration and Stem Cell Programs, Institute for Cell Engineering, Johns Hopkins University School of Medicine, Baltimore, MD, United States, [2]Department of Neuroscience, Johns Hopkins University School of Medicine, Baltimore, MD, United States, [3]Department of Biomedical Engineering, Johns Hopkins University School of Medicine, Baltimore, MD, United States, [4]Department of Neurology, Johns Hopkins University School of Medicine, Baltimore, MD, United States

The aggregation of α-synuclein in the nervous system leads to a class of neurodegenerative disorders termed α-synucleinopathies. A form of primary degenerative dementia called Lewy body dementia (LBD) often develops when these aggregations develop into intracellular inclusions called Lewy bodies (LB) and Lewy neurites (LN). Although high frequency of LBD are the leading cause of dementia after Alzheimer's disease (AD), limited information has been discovered about its pathological pathway or diagnostic criteria. In this report, we attempt to address such shortcomings via utilizing a proteomic approach to identify the proteome changes following intrastriatal injection of α-synuclein pre-formed fibril (α-syn PFF). Using mass spectrometry, we have identified a total of 179 proteins that were either up- or down-regulated at different time points, with the four proteins—TPP3, RAB10, CAMK2A, and DYNLL1, displaying the most significant changes throughout the timeframe. Through further examining the modulated proteins with network-based enrichment analyses, we have found that (1) the most significantly associated neurodegenerative pathways were Parkinson's ($pV = 3.0e\text{-}16$) and Huntington's ($pV = 1.9e\text{-}15$) disease, and (2) the majority of molecular functions specific to the pathology only appeared at later time points. While these results do not expose a conclusive biomarker for LBD, they suggest a framework that is potentially applicable to diagnose and differentiate LBD pathology from other forms of dementia by focusing on the cortical proteome changes which occur in a later time span.

KEYWORDS

Parkinson's Disease with Dementia, Lewy body dementia (LBD), quantitative proteomics, TMT-isobaric mass technique, synucleinopathy models

Introduction

α-synucleinopathies are a class of neurodegenerative disorders characterized by insoluble fibrillary aggregations of α-synuclein inside the cytoplasm of neurons and glial cells (Fujiwara et al., 2002; Jellinger, 2003; Marti et al., 2003; Lee et al., 2008). Neuronal inclusions, known as Lewy bodies (LB) and Lewy neurites (LN),

they lead to a subclass of disorders called Lewy body diseases which include Dementia with Lewy bodies (DLB), Parkinson's disease (PD), and Parkinson's Disease with Dementia (PDD) (Mueller et al., 2017; Surendranathan et al., 2020). Although the Lewy body dementias (LBD)—comprised of DLB and PDD are presumed to be the second most frequent cause of primary degenerative dementia following Alzheimer's Disease (AD), their exact clinical diagnosis and prevalence, especially for DLB, remain relatively unclear due to its concurrence or similarities with other types of dementia (Mueller et al., 2017; Kane et al., 2018; Matar et al., 2020). Thus, establishing clear clinical features and reliable diagnostic biomarkers for LBD have long been of interest in the field of neurology, with the international consensus criteria for DLB being revised four times since its foundation in 1996 (Yamada et al., 2020). Unlike the pathology of AD which involves the deposit of amyloid-β plaques in the cholinergic system and hippocampus, such areas are relatively spared in the case of DLB, in which Lewy bodies spread to the cortical/subcortical pathways (Gibb et al., 1987, 1989; Armstrong, 2020). Yet, due to its history of misdiagnoses and ambiguity, there is a relative deficit in data dedicated to identifying biomarkers or pathological conditions for the disease. Discovering progressive proteomic changes indicative of LBD will be critical in developing early diagnostic kits, a key component in ensuring the effectiveness of most treatments and medication. In this study, we utilize α-Synuclein pre-formed fibrils (α-syn PFF)—injected mice models to analyze proteomic changes at different time points following injection, attempting to elucidate the pathway and effects of α-Synuclein aggregation pathology.

Materials and methods

Preparation of α-syn PFF

To generate α-synuclein pre-formed fibrils (PFFs), monomeric mouse α-synuclein proteins were continuously agitated using a thermomixer (Eppendorf) at 1,000 rpm and 37°C for 7 days. Following this incubation, the fibrils were sonicated for 30 s at 10% amplitude, with a 0.5-s on/off pulse cycle (Branson Digital Sonifier), before use.

Intrastriatal injection of α-syn PFF

C57BL/6 WT mice purchased from the Jackson Laboratories (Bar Harbor, ME, USA) used in experiments. Mice were anesthetized with isoflurane (1%−2% inhalation), and small incision was made to expose the cranium. α-syn PFF is injected into the striatum of 2-month-old mice [2 μl (total 5 μg α-syn PFF) per hemisphere at 0.4 μl/min]. The stereotaxic coordinates, relative to the bregma were anteroposterior (AP) = +0.2 mm, mediolateral (ML) = +2.0 mm, dorsoventral (DV) = +2.8 mm. After each injection was completed, the needle was maintained in position for 5 min. Following needle removal, the wound was closed with silk suture and antibiotic ointment was applied to the surgical site. Animal was gently warmed on a 37°C heating pad for 3–5 min and returned to their original nesting material.

Sample preparation and TMT labeling

The cerebral cortices for each time point were dissected and collected. The tissues were homogenized using a Dounce homogenizer with CHAPS lysis buffer (150 mM KCl, 50 mM HEPES pH = 7.4, 0.1% CHAPS, and 1 protease inhibitor cocktail tablet per 50 ml of buffer). Subsequently, samples were sonicated (30 s on/off for 10 times at 4°C water bath) and centrifuged (16,000 *g* on 4°C for 10 min). Protein concentrations of the supernatant were measured using the Bicinchoninic acid assay (Pierce, Waltham, MA, USA). Reducing of cysteine chains from equal amounts of proteins (0.5 mg per condition) were performed using 5 mM DTT at 55°C for 60 min and alkylated using 5 mM iodoacetamide for 45 min at room temperature (RT) in the dark. The samples were then trypsinized for 3 h before Tandem mass tag (TMT) labeling. TMT labeling was carried out following as the manufacturer instructions (Dayon et al., 2008). Briefly, trypsinized peptides from four conditions were reconstituted in 50 mM TEABC buffer (2% SDS, 50 mM triethyl ammonium bicarbonate, 5 mM sodium fluoride, 1 mM sodium orthovanadate, and 1 mM β-glycerophosphate) and mixed with the 0.8 mg of TMT reagent and incubated at RT for 1 h. After the labeling, all samples were pooled and desalted using Sep-Pak C18 cartridges.

Mass spectrometry

LTQ-Orbitrap Elite mass spectrometer (Thermo Electron, Bremen, Germany) coupled with Easy-nLC II nanoflow LC system (Thermo Scientific, Odense, Denmark) was applied to identify sequence of peptides and quantification. Briefly, the total of 2 μg pooled TMT-labeled peptides were reconstituted in 0.1% formic acid and loaded on an analytical column (75 μm × 50 cm) at a flow rate of 300 nl/min using a linear gradient of 10%−35% solvent B (0.1% formic acid in 95% acetonitrile) over 120 min. Data-dependent acquisition with full scans in 350–1,700 m/z range was carried out using an Orbitrap mass analyzer at a mass resolution of 120,000 at 400 m/z. The 15 most intense precursor ions from a survey scan were selected for MS/MS fragmentation using higher-energy collisional dissociation (HCD) fragmentation with 32% normalized collision energy and detected at a mass resolution of 30,000 at 400 m/z. Automatic gain control for full MS was set to 1×10^6 for MS and 5×10^4 ions for MS/MS with a maximum ion injection time of 100 ms. Dynamic exclusion was set to 30 s. and singly charged ions were rejected. Internal calibration was carried out using the lock mass option (m/z 445.1200025) in ambient air.

Immunoblot assay

Samples were separated by 8%−16% SDS-PAGE and transferred to nitrocellulose membrane (0.45 μm). The membrane were incubated with PBS-T (0.05 % Tween 20, v/v) containing bovine serum albumin (5%, w/v) for blocking, and the membranes were applied with antibodies; polyclonal rabbit anti-TPPP3 (15057-1-AP, ProteinTech), polyclonal rabbit anti-RAB10 (11808-1-AP, ProteinTech), polyclonal rabbit anti-CaMKII-α (3357, Cell

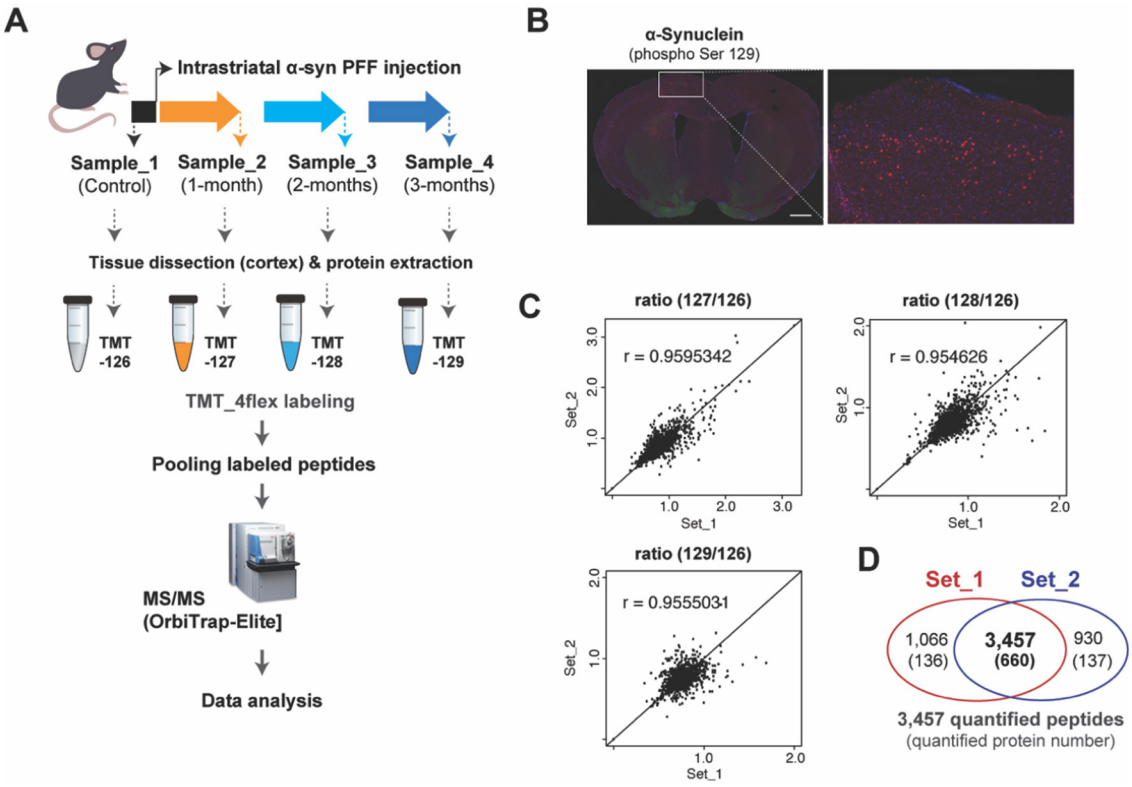

FIGURE 1
TMT-based protein quantification using α-syn PFF-injected mouse brain tissues. **(A)** Experimental illustration for the procedures of quantitative proteomics approaches including intrastriatal injection of α-syn PFF, sampling, TMT-labeling, and mass spectrometry is shown. **(B)** Representative immuno-stained images of coronal sections after 2 months of α-syn PFF injection using phospho-S129 α-synuclein antibody (red), indicating biodistribution and aggregation of α-syn PFF. Scale bars: 1 mm. **(C)** Scatter plots showing the reproducibility of transcriptomic data between biological replications of Set_1 and Set_2. **(D)** The Venn diagram indicates the overlapped number of peptides and proteins between two data of our biological replications obtained by TMT-based protein quantification.

Signaling Technology), polyclonal rabbit anti-DYNLL1 (A53885, EpigenTek), and rabbit anti-beta-Actin HRP conjugate (13E5, Cell Signaling Technology). Horseradish peroxidase-conjugated secondary anti-rabbit or anti-mouse IgG (Amersham Bioscience) was used to detecte in X-ray film (AGFA) by an ECL method (Thermo Scientific). Densitometry was performed by Image J, and values were averaged from three-independent experiments.

Data analysis

Cytoscape v3.9.1 software with the GlueGo v2.5.7 and BiNGO v3.0.3 plugins, coupled with reference networks such as KEGG, Gene Ontology (GO): Biological Process (BP) and Molecular Function (MF) resources were applied by according to the instruction manual (Maere et al., 2005; Bindea et al., 2009).

Statistical analysis

Quantitative data were presented as mean ± SEM using GraphPad prism software with unpaired student's *t*-test. Statistic approaches for functional analysis: ClueGO and BiNGO were assessed by the Two-sided hypergeometric test coupled with the Bonferroni step-down for correction and hypergeometric test coupled with Benjamini&Hochberg False Discovery Rate (FDR) correction respectively.

TABLE 1 Thirty-seven proteins (AVR > 5% up-regulated; Group A) had significance among 186 up-regulated proteins, and 142 proteins (AVR > 20% down-regulated; Group B) had significance among 473 down-regulated proteins.

Nr. of total protein	Nr. of up-regulated proteins (AVR > 5%)	Nr. of down-regulated proteins (AVR > 20%)
660	37 (Group A)	142 (Group B)
Group C (179 proteins) = Group A + Group B		

One hundred seventy-nine proteins (Group C = Group A + B) were used for functional network analysis.

Results

Quantitative proteomic screening for α-syn PFF-injected mouse brain tissues

A high-throughput proteomic profiling was performed to identify large-scale proteome changes following intrastriatal injection of α-synuclein pre-formed fibril (α-syn PFF) in C57BL6

10.3389/frdem.2024.1477986

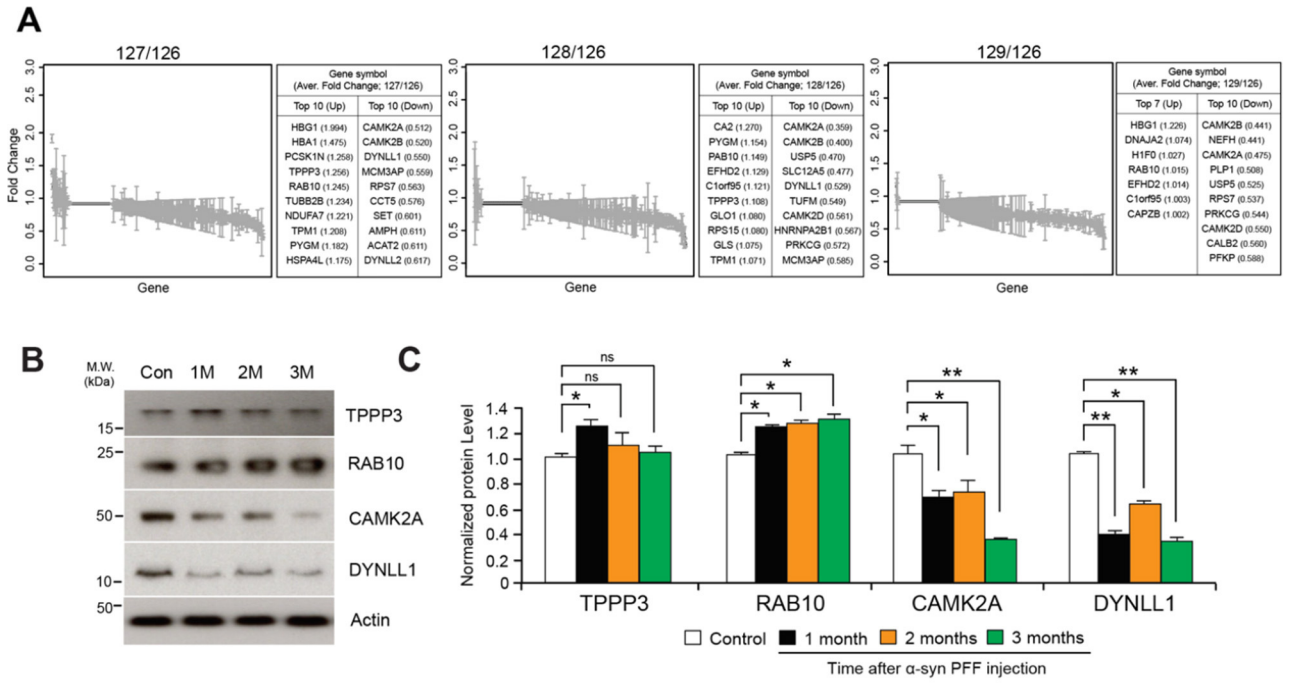

FIGURE 2
Protein quantification using TMT-labeled peptides. **(A)** Fold changes of 660 commonly identified proteins after normalization using peptides with expression of mass reporter (126 Da). **(B)** Western blot validation of significantly up- and down-regulated proteins including Tubulin polymerization-promoting protein family member 3 (TPPP3), Ras-related protein Rab-10 (RAB10), Calcium/calmodulin-dependent protein kinase type II subunit alpha (CAMK2A), Dynein light chain 1 (DYNLL1). **(C)** Quantification graphs of expression ratio obtained from triplicate samples and normalized using expression of β-Actin; two-tailed unpaired Student's *t*-test. $*p < 0.05$, $**p < 0.01$, n.s., not significant from Student's *t*-test.

mice (Figure 1A). After injecting α-syn PFF on eight male mice per time point, six mice were sacrificed and grouped into Set_1 and Set_2 ($n = 3$ mice per set with biological replication) for proteomic profiling, and the remaining mice were used for immunostaining to check the propagation of α-syn PFF. α-syn PFF was stably injected, distributed to cerebral cortex, and aggregated in cerebral cortex at 2-months as evidenced by immunostaining using anti-phospho-S129 α-synuclein antibody (Figure 1B). Two sets of quantitative proteomic screening using Tandem mass tag (TMT) technique were compared for reliability, whose results are illustrated in Figure 1C. A regression analysis of sample ratios revealed a strong positive correlation between Set_1 and Set_2 (Figure 1C). For Set_1 and Set_2, the number of quantified peptides were 4,523 and 4,387, with 3,457 shared (76.4% and 78.8%, respectively) between the two sets; the number of quantified protein groups were 796 and 797, with 660 shared (82.9 and 82.8%, respectively; Figure 1D, Supplementary Table S1). Among the 660 shared protein groups, 37 were classified as up-regulated (AVR >5%) and 142 as down-regulated (AVR >20%; Table 1 and Supplementary Table S2).

Functional alteration following intrastriatal α-syn PFF injection

A comparative analysis of average fold changes relative to the control revealed changes in gene expression over time by Proteome Discoverer v1.4, with a range of up- and down-regulated proteins after 1-, 2-, and 3-month following α-syn PFF injection (Figure 2A, Supplementary Table S2). The four most prominent alterations presented in all three time points included the upregulation of Tubulin polymerization promoting protein family member 3 (TPPP3) and Ras-related protein Rab-10 (RAB10), and the downregulation of Calcium/calmodulin dependent protein kinase II alpha (CAMK2A) and Dynein light chain 1 (DYNLL1). All changes were statistically significant with the exception of TPPP3 at 2 and 3 months (Figures 2B, C).

Network-based KEGG and GO: biological process analysis

The network analysis of significantly up- and down-regulated proteins identified several enriched Kyoto Encyclopedia of Genes and Genomes (KEGG) pathways and GO biological processes (BP), designated by a minimum association of 6% or 8% of genes and *p*-value < 1.0e-5 (Figures 3A, B). Total 17 representative pathways spanning over a wide range of networks for metabolism, environmental information processing, cellular processes, organismal systems, and human diseases were discovered in KEGG pathways (Figure 1A, Supplementary Table S3). The pathways with the greatest significance were neurodegenerative disorders including Parkinson's ($pV = 3.0e-16$) and Huntington's ($pV = 1.9e-15$) disease, endocrine and other factor-regulated calcium reabsorption ($pV = 8.8e-14$), and synaptic vesicle cycle ($pV =$

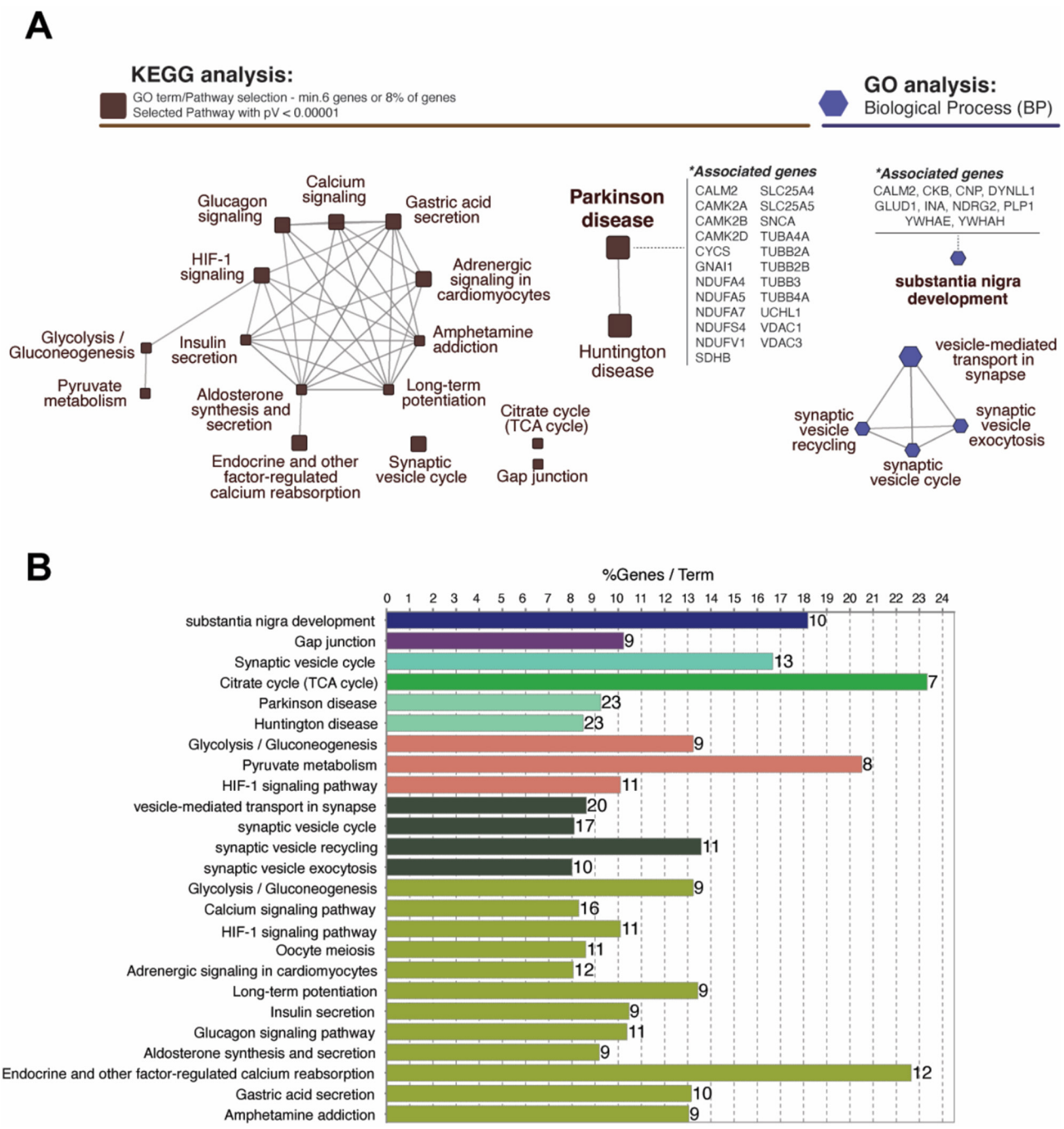

FIGURE 3
Analysis of functional networks using ClueGo Cytoscape plugin. **(A)** Network-based KEGG and GO analysis represent proteins classified into specific pathways which are labeled beside the nodes. Total 17 representative pathways with a high significance ($pV < 0.00001$) including Parkinson's (23 genes; 9.24%) and Huntington diseases (23 genes; 8.49%) were identified in KEGG pathways. GO:Biological Process analysis identified five enriched networks including substantia nigra development (10 genes; 18.18%). **(B)** Bar graph represents the number of genes, terms, and %geneset in each pathway shown in **(A)**. *$p < 0.05$.

5.6e-13) (Supplementary Table S3). GO analysis elucidated five networks displaying high significance, including vesicle-mediated transport (pV = 1.1e-13) and substantia nigra development (pV = 1.1e-10). The relative p-values and percentage per number of associated genes for all KEGG pathways and GO: BP are depicted in Figure 3B.

Time-dependent network-based GO: molecular function analysis

Additionally, a network-based GO: molecular function (MF) analysis was performed to investigate the molecular progression of α-Synuclein aggregates in significantly up- and down-regulated

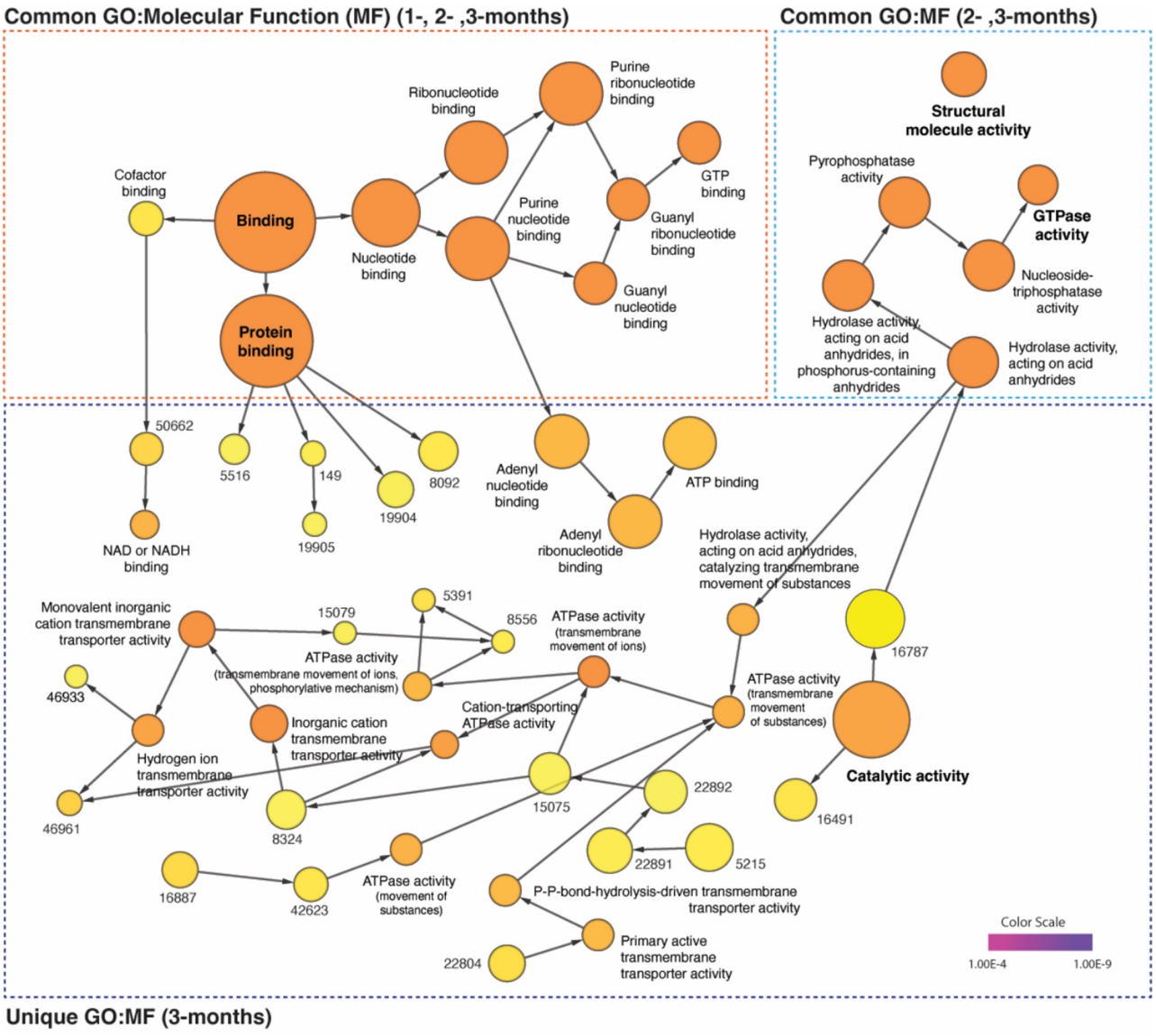

FIGURE 4
Distinct time-dependent GO profiles and network dynamics in post-α-syn PFF-injection. The gene ontology (GO) enrichment analysis of up- (AVR > 5%) and down-regulated (AVR > 20%) proteins in each time points were performed on the network using BiNGO plugin of Cytoscape (v.3.9.1). The common and unique clusters of molecular function (MF) were shown. The color gradient of the cluster distribution stands for the *p*-value of each cluster associated with the term. Darker (orange) color indicates a lower *p*-value. Numbers on yellow color (relevantly higher *p*-value) indicate GO-ID number, which provided in Supplementary Table S4.

proteins for the three time points of interest. We found that the number of significantly ($pV < 1.0e-5$) enriched GO: MF clusters increased over time, with 37 unique clusters including ATPase ($pV = 8.9e-11$) and Catalytic ($pV = 8.1e-9$) activity only appearing at 3 months after α-syn PFF injection. Nevertheless, the most significant and frequent clusters appeared to be those common across multiple time points, such as nucleotide ($pV = 1.2e-20$ at 3-month) and protein ($pV = 1.3e-17$) binding present at 1-, 2-, and 3-month, and GTPase activity ($pV = 4.3e-15$) present at 2- and 3-month. Information regarding *p*-values, cluster frequency, and associated genes for all significantly enriched functions are provided in Figure 4 and Supplementary Table S4.

Discussion

In this study, we used a proteomic approach in the mouse brain to elucidate the pathological pathways and mechanisms associated with α-synuclein propagation which often leads to Lewy body dementias (LBD) in human patients. Previous literature has discovered that while Lewy bodies originate in the substantia nigra, their ascension to the cortex is the pathway lying behind Parkinson's disease and Dementia with Lewy bodies (Obeso et al., 2010). Consistent with this theory, we have observed α-synuclein aggregations in the mouse cortex through coronal sections, supporting the clinical relevance of the study for human models. Investigating the range of varying gene expression levels through

mass spectrometry analysis, we have identified several genes which were commonly altered at all time points after α-syn PFF injection, including TPPP3 and RAB10, which were upregulated, and CAMK2A and DYNLL1, which were downregulated. TPPP3 regulates microtubule stability and may contribute to α-synuclein aggregation, a key feature of PDD. DYNLL1 and RAB10 play essential roles in intracellular transport and protein clearance, processes that, when dysregulated, lead to neuronal toxicity and degeneration. The role of CAMK2A in calcium homeostasis links to neurotoxicity and the loss of neurons (Ghosh and Giese, 2015; Zhang et al., 2014; Olah et al., 2020; Fellgett et al., 2021). These results agree with prior reports on neurodegenerative diseases, where all four genes displaying association with not only Parkinson's (Simunovic et al., 2009; Zhang et al., 2014; Olah et al., 2020; Fellgett et al., 2021), but also with Alzheimer's (Kong et al., 2009; Ghosh and Giese, 2015; Ridge et al., 2017; Singh et al., 2022) disease. Thus, while we may conclude that these genes may serve as potential biomarkers for early detection of general neurodegeneration, it appears difficult to assign them to a particular diagnosis.

Our network-based analysis suggests a method to differentiate specific pathologies from similar disorders by identifying differences in associated genes and enriched pathways/molecular functions at various time points. For instance, the same number of genes with modified expression were associated with the enrichment of both Parkinson's and Huntington's disease pathways via KEGG analysis, with the majority of genes shared between the two. However, the deciding factor between these two similar motor disorders was that the unshared genes for Parkinson's disease were related to calcium-dependent signaling (CAMK2- α, β, δ), while those for Huntington's disease were related to adaptor protein complexes (AP2- α1, β1, Mu1). Additionally, our GO:MF analysis revealed that calmodulin binding was only enriched 2 and 3 months after α-syn PFF injection. We believe this implies that while the two diseases may share common signatures early on during their progression, the detailed pathways appearing over time, in this case the calcium/calmodulin-dependent pathways, may serve as a diagnosis criterion in distinguishing a specific condition. Performing time-dependent GO or KEGG pathway analysis allows researchers to capture dynamic biological responses and track disease progression over time. It helps identify temporal patterns in biological processes, distinguishing early, mid, and late-stage responses, and can highlight critical time points for effective therapeutic intervention as well as refining stage-specific biomarkers. This idea is further strengthened by the fact that while a relatively small number (11 modules) of general, significant functions emerged at 1-month, a large number (53 modules) of uncommon, specific functions emerged at 3 months.

Being one of the first of its kind, our study illustrates the possibility of utilizing a proteomic approach in identifying Lewy-body related neurodegeneration. However, it is also not without its limitations. First, while the human neurodegenerative dementias develop gradually over a prolonged timeframe of years, our analysis studied differences in gene expression over 3 months. Thus, the definitive signatures in human models may differ significantly from those in our report. Additionally, due to the lack of similar studies, the verification of the potential biomarkers we identified remains a challenge.

Data availability statement

The datasets presented in this study can be found in online repositories. The names of the repository/repositories and accession number(s) can be found in the article/Supplementary material.

Ethics statement

All experimental protocols using animals were approved by and conformed to the Institutional Animal Care and Use committee of the Johns Hopkins University. The study was conducted in accordance with the local legislation and institutional requirements.

Author contributions

FA: Conceptualization, Data curation, Investigation, Methodology, Visualization, Writing – original draft. IJ: Conceptualization, Investigation, Software, Writing – original draft, Writing – review & editing. YC: Conceptualization, Data curation, Investigation, Methodology, Validation, Writing – original draft, Writing – review & editing. YM: Data curation, Investigation, Validation, Writing – review & editing. JP: Data curation, Formal analysis, Resources, Software, Visualization, Writing – review & editing. HJ: Investigation, Methodology, Supervision, Writing – review & editing. LK: Data curation, Formal analysis, Investigation, Writing – review & editing. AM: Investigation, Validation, Visualization, Writing – review & editing. BB: Data curation, Investigation, Resources, Software, Writing – review & editing. DY: Investigation, Validation, Writing – review & editing. JX: Conceptualization, Project administration, Supervision, Writing – original draft, Writing – review & editing. CN: Conceptualization, Data curation, Formal analysis, Funding acquisition, Investigation, Project administration, Resources, Software, Supervision, Writing – original draft, Writing – review & editing. S-UK: Conceptualization, Funding acquisition, Project administration, Supervision, Visualization, Writing – original draft, Writing – review & editing.

Funding

The author(s) declare financial support was received for the research, authorship, and/or publication of this article. This work was supported by the National Institutes of Health (NIH)/National Institute of Neurological Disorders and Stroke (NINDS) R01 NS123456.

Conflict of interest

The authors declare that the research was conducted in the absence of any commercial or financial relationships that could be construed as a potential conflict of interest.

The author(s) declared that they were an editorial board member of Frontiers, at the time of submission. This had no impact on the peer review process and the final decision.

Publisher's note

All claims expressed in this article are solely those of the authors and do not necessarily represent those of their affiliated organizations, or those of the publisher, the editors and the reviewers. Any product that may be evaluated in this article, or claim that may be made by its manufacturer, is not guaranteed or endorsed by the publisher.

Supplementary material

The Supplementary Material for this article can be found online at: https://www.frontiersin.org/articles/10.3389/frdem.2024.1477986/full#supplementary-material

References

Armstrong, R. (2020). What causes neurodegenerative disease? *Folia Neuropathol.* 58, 93–112. doi: 10.5114/fn.2020.96707

Bindea, G., Mlecnik, B., Hackl, H., Charoentong, P., Tosolini, M., Kirilovsky, A., et al. (2009). ClueGO: a cytoscape plug-in to decipher functionally grouped gene ontology and pathway annotation networks. *Bioinformatics* 25, 1091–1093. doi: 10.1093/bioinformatics/btp101

Dayon, L., Hainard, A., Licker, V., Turck, N., Kuhn, K., Hochstrasser, D. F., et al. (2008). Relative quantification of proteins in human cerebrospinal fluids by MS/MS using 6-plex isobaric tags. *Anal. Chem.* 80, 2921–2931. doi: 10.1021/ac702422x

Fellgett, A., Middleton, C. A., Munns, J., Ugbode, C., Jaciuch, D., Wilson, L. G., et al. (2021). Multiple pathways of LRRK2-G2019S/Rab10 interaction in dopaminergic neurons. *J. Parkinsons Dis.* 11, 1805–1820. doi: 10.3233/JPD-202421

Fujiwara, H., Hasegawa, M., Dohmae, N., Kawashima, A., Masliah, E., Goldberg, M. S., et al. (2002). Alpha-synuclein is phosphorylated in synucleinopathy lesions. *Nat. Cell. Biol.* 4, 160–164. doi: 10.1038/ncb748

Ghosh, A., and Giese, K. P. (2015). Calcium/calmodulin-dependent kinase II and Alzheimer's disease. *Mol. Brain* 8:78. doi: 10.1186/s13041-015-0166-2

Gibb, W. R., Esiri, M. M., and Lees, A. J. (1987). Clinical and pathological features of diffuse cortical Lewy body disease (Lewy body dementia). *Brain* 110, 1131–1153. doi: 10.1093/brain/110.5.1131

Gibb, W. R., Mountjoy, C. Q., Mann, D. M., and Lees, A. J. (1989). A pathological study of the association between Lewy body disease and Alzheimer's disease. *J. Neurol. Neurosurg. Psychiatry* 52, 701–708. doi: 10.1136/jnnp.52.6.701

Jellinger, K. A. (2003). Neuropathological spectrum of synucleinopathies. *Mov. Disord.* 18(Suppl 6), S2–S12. doi: 10.1002/mds.10557

Kane, J. P. M., Surendranathan, A., Bentley, A., Barker, S. A. H., Taylor, J. P., Thomas, A. J., et al. (2018). Clinical prevalence of Lewy body dementia. *Alzheimers Res. Ther.* 10:19. doi: 10.1186/s13195-018-0350-6

Kong, W., Mou, X., Liu, Q., Chen, Z., Vanderburg, C. R., Rogers, J. T., et al. (2009). Independent component analysis of Alzheimer's DNA microarray gene expression data. *Mol Neurodegener* 4:5. doi: 10.1186/1750-1326-4-5

Lee, H. J., Suk, J. E., Bae, E. J., and Lee, S. J. (2008). Clearance and deposition of extracellular alpha-synuclein aggregates in microglia. *Biochem. Biophys. Res. Commun.* 372, 423–428. doi: 10.1016/j.bbrc.2008.05.045

Maere, S., Heymans, K., and Kuiper, M. (2005). BiNGO: a Cytoscape plugin to assess overrepresentation of gene ontology categories in biological networks. *Bioinformatics* 21, 3448–3449. doi: 10.1093/bioinformatics/bti551

Marti, M. J., Tolosa, E., and Campdelacreu, J. (2003). Clinical overview of the synucleinopathies. . *Disord.* 18(Suppl 6), S21–S27. doi: 10.1002/mds.10559

Matar, E., Ehgoetz Martens, K. A., Halliday, G. M., and Lewis, S. J. G. (2020). Clinical features of Lewy body dementia: insights into diagnosis and pathophysiology. *J. Neurol.* 267, 380–389. doi: 10.1007/s00415-019-09583-8

Mueller, C., Ballard, C., Corbett, A., and Aarsland, D. (2017). The prognosis of dementia with Lewy bodies. *Lancet Neurol.* 16, 390–398. doi: 10.1016/S1474-4422(17)30074-1

Obeso, J. A., Rodriguez-Oroz, M. C., Goetz, C. G., Marin, C., Kordower, J. H., Rodriguez, M., et al. (2010). Missing pieces in the Parkinson's disease puzzle. *Nat. Med.* 16, 653–661. doi: 10.1038/nm.2165

Olah, J., Lehotzky, A., Szunyogh, S., Szenasi, T., Orosz, F., Ovadi, J., et al. (2020). Microtubule-associated proteins with regulatory functions by day and pathological potency at night. *Cells* 9:357. doi: 10.3390/cells9020357

Ridge, P. G., Karch, C. M., Hsu, S., Arano, I., Teerlink, C. C., Ebbert, M. T. W., et al. (2017). Linkage, whole genome sequence, and biological data implicate variants in RAB10 in Alzheimer's disease resilience. *Genome Med.* 9:100. doi: 10.1186/s13073-017-0486-1

Simunovic, F., Yi, M., Wang, Y., Macey, L., Brown, L. T., Krichevsky, A. M., et al. (2009). Gene expression profiling of substantia nigra dopamine neurons: further insights into Parkinson's disease pathology. *Brain* 132(Pt 7), 1795–1809. doi: 10.1093/brain/awn323

Singh, H. N., Swarup, V., Dubey, N. K., Jha, N. K., Singh, A. K., Lo, W. C., et al. (2022). Differential transcriptome profiling unveils novel deregulated gene signatures involved in pathogenesis of Alzheimer's disease. *Biomedicines* 10:611. doi: 10.3390/biomedicines10030611

Surendranathan, A., Kane, J. P. M., Bentley, A., Barker, S. A. H., Taylor, J. P., Thomas, A. J., et al. (2020). Clinical diagnosis of Lewy body dementia. *BJPsych Open* 6:e61. doi: 10.1192/bjo.2020.44

Yamada, M., Komatsu, J., Nakamura, K., Sakai, K., Samuraki-Yokohama, M., Nakajima, K., et al. (2020). Diagnostic criteria for dementia with lewy bodies: updates and future directions. *J. Mov. Disord.* 13, 1–10. doi: 10.14802/jmd.19052

Zhang, S., Xie, C., Wang, Q., and Liu, Z. (2014). Interactions of CaMKII with dopamine D2 receptors: roles in levodopa-induced dyskinesia in 6-hydroxydopamine lesioned Parkinson's rats. *Sci. Rep.* 4:6811. doi: 10.1038/srep06811